Title page

1) Authors' names

Yoshimasa Kubota,[1] Hiroshi Kawakami,[1] Mitsuteru Natsuizaka,[1] Kazumichi Kawakubo,[1] Katsuji Marukawa,[2] Taiki Kudo,[1] Yoko Abe,[1] Kimitoshi Kubo,[1] Masaki Kuwatani,[1] Yutaka Hatanaka,[2] Tomoko Mitsuhashi,[2] Yoshihiro Matsuno,[2] Naoya Sakamoto[1]

2) Article title

CTNNB1 mutational analysis of solid-pseudopapillary neoplasms of the pancreas using EUS-guided fine-needle aspiration and next-generation deep sequencing

3) Authors' current affiliations

[1] Department of Gastroenterology and Hepatology, Hokkaido University Graduate School of Medicine, Sapporo, Japan

[2] Department of Surgical Pathology, Hokkaido University Hospital, Sapporo, Japan

4) Corresponding author information

Hiroshi Kawakami, MD, PhD,

Kita-15, Nishi-7, Kita-ku, Sapporo 060-8638, Japan

Business telephone: +81-11-706-7715

Fax: +81-11-706-7867

E-mail: hiropon@med.hokudai.ac.jp

5) Short title

Mutational analysis of SPN using EUS-FNA and NGS

6) Word count

2,415 words

Abstract:

Background: Solid-pseudopapillary neoplasm (SPN), a rare neoplasm of the pancreas, frequently harbors mutations in exon3 of the cadherin-associated protein beta 1 (*CTNNB1*) gene. Here, we analyzed SPN tissue for *CTNNB1* mutations by deep sequencing using next-generation sequencing (NGS).

Methods: Tissue samples from 7 SPNs and 31 other pancreatic lesions (16 pancreatic ductal adenocarcinomas [PDAC], 11 pancreatic neuroendocrine tumors [PNET], 1 acinar cell carcinoma, 1 autoimmune pancreatitis lesion, and 2 focal pancreatitis lesions) were analyzed by NGS for mutations in exon3 of *CTNNB1*.

Results: A single-base pair missense mutations in exon3 of *CTNNB1* was observed in all 7 SPNs and in 1 of 11 PNET samples. However, mutations were not observed in the tissue samples of any of the 16 PDAC or other 4 pancreatic disease cases. The variant frequency of *CTNNB1* ranged from 5.4% to 48.8%.

Conclusions: Mutational analysis of *CTNNB1* by NGS is feasible and was achieved using SPN samples obtained by EUS-FNA.

Keywords:

CTNNB1, solid-pseudopapillary neoplasms of the pancreas, endoscopic ultrasound-guided fine-needle aspiration, next-generation sequencing

Introduction

Solid-pseudopapillary neoplasm (SPN) of the pancreas is a rare tumor that accounts for 0.2–2.7% of all pancreatic tumors[1], predominantly seen in young female patients. It was first described by Frantz[2] in 1959. SPN of the pancreas is characterized by low-grade malignant potential, with an incidence of metastasis of 15%, and tends to have a favorable prognosis with surgical resections, considered the standard of care, with a 5-year overall survival rate of more than 95%[1,3,4].

ß-catenin is one of a submembranous component of the cadherin-mediated cell adhesion system and acts as a downstream transcriptional activator of Wnt signaling. Under normal conditions, cytoplasmic ß-catenin is expressed at a low level. Phosphorylation of both adenomatous polyposis coli (APC) and axin by glycogen synthase kinase-3ß (GSK-3ß) enhances ß-catenin binding to the APC-axin complex and targets the protein for ubiquitination and proteasomal degradation[5]. In the nucleus, ß-catenin forms complexes with proteins such as Tcf and Lef-1[6] and activates the transcription of several oncogenic genes including c-myc and cyclin D1.

Mutations in exon 3 of the ß-catenin gene (also called *CTNNB1*) are reported in approximately 83–100%[7-12] of surgically resected SPN samples. Accordingly, these mutations are considered a unique genetic characteristic of SPNs, differentiating them from other pancreatic tumors.

Direct sequencing is considered the gold standard for mutational analysis. However, it is difficult to detect a small proportion of mutant genes using this method. Recently, next-generation sequencing (NGS) has enabled the evaluation of multiple genes for genomic alterations in a single tumor, with high accuracy[13]. Less frequent mutations can also be detected if deep sequencing is performed.

Several studies have described the usefulness of EUS-guided fine-needle aspiration (EUS-FNA) for diagnosing SPNs[14-18]. SPNs could be seen as well-demarcated, hypoechoic, solid masses that sometimes coexist with cystic lesions and/or calcification on EUS. Accuracy of preoperative SPN diagnosis by EUS-FNA is reported to be 75–100%[17,18]; however, diagnosis by EUS-FNA is sometimes difficult because of interpretative, sampling, and misclassification errors or insufficient material for immunostaining[19]. In addition, EUS-FNA samples sometimes contain tumor cells that are too small to use for sequencing analysis by polymerase chain reaction (PCR)-based direct sequencing.

In the present study, we analyzed *CTNNB1* mutations using EUS-FNA samples and NGS. To the best of our knowledge, this is the first report of *CTNNB1* mutational analysis using EUS-FNA samples and NGS.

Methods

Samples: Thirty-eight samples were tested: 7 SPNs, 16 pancreatic ductal

adenocarcinomas (PDAC), 11 pancreatic neuroendocrine tumors (PNET), and 4 other pancreatic lesions. Non-SPN samples were used as controls. Samples were obtained by either EUS-FNA (n = 31) or surgery (n = 2) at Hokkaido University Hospital, Sapporo, Japan, between December 2008 and June 2013. All participants provided written informed consent, and the ethics committee at Hokkaido University Graduate School of Medicine approved the study.

EUS-FNA procedure: EUS-FNA was performed by a single experienced endoscopist (H.K.) using a curvilinear echoendoscope (GF-UCT240-AL5; Olympus Medical Systems Co., Tokyo, Japan) and 22-gauge needles (Echotip Ultra; Cook Japan, Tokyo, Japan) under conscious sedation. Briefly, the lesions were visualized by EUS, and the needle was advanced into the lesion through the gastric or duodenal wall. The central stylet was removed, and a syringe was attached to the needle hub to apply negative suction pressure. The needle was then moved back and forth within the lesion at least 10 times and then removed through the scope, before the stylet was re-inserted into the needle. The specimen obtained by aspiration was placed on a slide, air-dried, alcohol-fixed, and used to prepare smears that were stained using the rapid Romanowsky technique for quick interpretation and assessment of sample adequacy (Diff-Quik stain; Kokusai Shiyaku, Kobe, Japan). Diff-Quik staining was performed on all specimens by an experienced cytotechnologist (K.M.). Cytological and histological diagnoses were made for the specimens obtained by EUS-FNA[20,21].

DNA extraction, PCR, and sequencing analysis of CTNNB1: The FNA samples were stored in RNAlater (Life Technologies Corporation, Carlsbad, CA). Genomic DNA and RNA were extracted from samples using an AllPrep® DNA/RNA/Protein mini kit (Qiagen, Inc., Valencia CA) according to the manufacturer instructions. Three PNET samples were obtained from surgery. Tumor samples were fixed in 10% buffered formalin and embedded in paraffin for microdissection of the tumor tissue. Genomic DNA was semi-automatically extracted using QIAamp® DNA FFPE tissue kit (Qiagen) and QIAcube® (Qiagen) according to the manufacturer instructions. Total RNA concentration was determined by spectrophotometer (NanoDrop2000/2000c; Thermo Scientific, Tokyo, Japan), and 5 µg total RNA was reverse transcribed using SuperScript® II Reverse Transcriptase (Invitrogen, Carlsbad, CA). Approximately 100ng of each genomic DNA sample was used for PCR. Genomic DNA was amplified by semi-nested PCR, using the first and second primer pairs (*Table 1*). Primers for the second PCR contained adaptors and barcodes for further NGS analysis, and the PCR products were bidirectionally read by NGS. These primers were designed to amplify a 228-bp DNA fragment of entire exon 3 of *CTNNB1*. The thermal cycler (Life Technologies) was programmed as follows: initial denaturation at 94°C for 7 min and 35 amplification cycles for each PCR. Each amplification cycle comprised denaturation at 94°C for 15 s, annealing at 58°C for 15 s, and elongation at 72°C for 30 s. The last cycle was followed by a final extension at 72°C for 5 min. The PCR products were verified by agarose gel electrophoresis.

The band of the expected size was excised and purified using a QIAquick® Gel Extraction kit (Qiagen).

The concentration and amplicon size of the bar-coded libraries were determined by using an Agilent 2100 Bioanalyzer and Agilent DNA 1000 kit (Agilent Technologies, Inc., Santa Clara CA).

They were pooled and mixed with Ion Spheres™ particles for emulsion PCR using the Ion OneTouch™ System (Life Technologies) with an Ion OneTouch™ Template kit v2 (Life Technologies) according to the manufacturer instructions. Samples were subsequently enriched using Ion OneTouch™ ES (Life Technologies). The final concentration of the template for emulsion PCR was 0.4 pM. Sequencing was performed on an Ion PGM™ (Personal Genome Machine) Sequencer by using an Ion 314™ chip (Life Technologies) with an IonPGM™ Sequencing 200 kit (Life Technologies) according to the manufacturer protocol. Obtained sequences were mapped onto the human reference genome hg19, and variants were detected using Ion Torrent Suite v2.2 software (Life Technologies).

The PCR products were also submitted to direct sequencing using ABI Big Dye Terminator v1.1 Cycle Sequencing Kit (Applied Biosystems, Foster City, CA) and the primers used for PCR. Sequencing of each PCR product was performed with ABI PRISM™ 310 Genetic Analyzer (Applied Biosystems). Each mutation was verified in both sence/antisence directions.

Results

Clinicopathological features

The clinicopathological features of the 38 patients are summarized in Table 2. The patient population comprised 24 women and 14 men, with ages ranging from 13 to 81 years (median: 63.5 years). SPNs tended to be located in the pancreatic body and tail rather than in the pancreatic head. Other tumors involved all parts of the pancreas and were evenly distributed. Tumor sizes ranged from 8 to 95 mm at the greatest diameter (median: 23 mm).

The types of surgical procedures were as follows: 3 subtotal stomach-preserving pancreaticoduodenectomies, 2 duodenum-preserving pancreas head resection, 7 distal pancreatectomies (4 with splenectomy and 1 with spleen and left adrenal gland resection), 1 partial pancreatectomy, and 1 left nephrectomy with metastatic lymph node tumor resection. Two patients with PDAC had resectable disease, whereas the other cases were unresectable.

The histological features of the specimens with SPN obtained by EUS-FNA are shown in Figure 1. In most cases, SPN showed typical findings, but in case 7, SPN was difficult to be distinguished from PNET. Immunohistochemical staining was performed for SPN and PNET samples. Two SPNs showed a few chromogranin A positive cells, 5 of 7 SPNs showed immunoreactivity against Synaptophysin, and 5 SPNs showed nuclear staining for ß-catenin. All PNET samples were positive for chromogranin A and synaptophysin, and none

showed nuclear immunoreactivity against ß-catenin.

Genomic DNA and RNA were extracted from FNA samples in 35 patients. For 3 PNET patients (Case 26, 27 and 31), surgically resected specimen were used to obtain DNA.

Mutations in exon3 of CTNNB1 by NGS

All 7 SPNs showed a single-base pair missense mutation in exon 3 of *CTNNB1*. Neither PDAC nor acinar cell carcinoma cases showed *CTNNB1* exon 3 mutation. Of the 11 PNETs, a single-base pair missense mutation was detected in 1 sample. Variant frequency and coverage ranged from 5.4% to 48.8% and from 4,490 to 203,919, respectively. For the sample with a variant frequency of 5.39, the read depth was 15,199. The involved codons were as follows: codon 32 (3 cases), codon 37 (2 cases), and codon 41 (3 cases). The results of the analysis are shown in Table 3. For the control samples, the average base coverage depth ranged from 113 to 8,027 (median: 7,312).

Mutations in exon3 of CTNNB1 by direct sequencing

Direct sequencing was performed using samples that had mutations detected by NGS. One SPN case with mutation was not able to perform direct sequencing due to insufficient amount of the sample. Only 1 of the 7 cases could detect mutation by direct sequencing as shown also in Table 3.

Discussion

Mutations in exon 3 of *CTNNB1* have been reported in various tumors, including those of the colon[22], prostate[23], endometrium[24], and liver[25].

In SPN, cytoplasmic/nuclear immunoreactivity for ß-catenin was detected during the systemic immunohistochemical study of pediatric tumors[7]. After the first report by Tanaka *et al.* [7], mutations in exon 3 of *CTNNB1* have been reported in 83–100% [7-12] of SPNs. Previous studies used microdissected tumor tissue from formalin-fixed, paraffin-embedded blocks obtained by surgery to extract genomic DNA. Single-base pair missense mutations in codons 32, 33, 34, 37, and 41 and 12-base pair deletion corresponding to codons 28 to 32 have been documented.

Serine 33 and 37 as well as threonine 41 are the sites for GSK-3 ß phosphorylation[26]. Codons 32 and 34 serve as crucial elements of the DSGΦXS motif to create a recognition site for ß-TrCP and subsequent ubiquitin-mediated proteasomal degradation[27,28]. Both mechanisms lead to the abnormal stabilization of ß -catenin and its resultant aberrant nuclear expression in SPNs.

In the present study, 8 cases showed *CTNNB1* mutations. Mutations were detected in codons 32, 37, and 41, finding consistent with previous reports[7-12]. To the best of our knowledge, this is the first report of mutational analysis for *CTNNB1* using EUS-FNA

samples and NGS. Of the 8 cases, 7 were of SPN and 1 was of PNET. That PNET was diagnosed by the typical radiologic finding (a hypervascular round mass that was best visualised in the arterial contrast enhancement phase on computed tomography) and immunohistochemical staining (positive chromogranin A and synaptophysin immunostaining, negative CD56 staining and no nuclear ß-catenin accumulation) of EUS-FNA sample. The patient did not undergo surgery because of the small size (9.6 × 5.4mm) and low-grade malignant potential of the lesion, which was diagnosed on the basis of EUS-FNA specimen analysis (Ki-67 index, 1–2%).

Several assays can be performed to detect genetic mutations, such as hematoxylin and eosin and immunohistochemical staining, fluorescence in situ hybridization, polymerase chain reaction, and direct sequencing. Although direct sequencing is considered the gold standard, it lacks the ability to detect small proportions of mutant genes and technical experience is essential for result interpretation. In one study, mutant DNA had to account for at least 30% of wild-type DNA for the detection of mutations by direct sequencing[29]. In our study, mutations caught by NGS could be detected in only 1 of 7 samples by direct sequencing. Our result showed superiority of NGS in detecting mutations than direct sequencing as in previous reports. Thus suggesting the usefulness of FNA specimen for genetic analyses when combined with NGS since EUS-FNA specimens are usually mixed with blood or tissue of needle tract.

To date, *CTNNB1* mutations have not been reported in PNET. Gerdes *et al.*[30] previously performed *CTNNB1* mutational analysis on 78 PDAC, 33 PNET and 14 pancreatic cancer cell lines and found no mutations in exon3 of *CTNNB1*. Similarly, Liu *et al.*[10] found no mutations in exon 3 of *CTNNB1* in 14 PNET samples. Exome sequence analysis of approximately 18,000 protein-coding genes of 10 PNET samples was carried out by Jiao *et al.*[31] to explore the genetic basis of the disease. They reported novel *DAXX* and *ATRX* mutations, but mutations in *CTNNB1* were not detected. With regard to neuroendocrine tumors in other organs, Kim *et al.*[32] detected a single-base pair mutation in 1 of 2 thymus neuroendocrine tumors, which resulted in a replacement of isoleucine by serine at codon 35. Another mutation was seen in a cell line of neuroendocrine tumor of midgut (terminal ileum) origin[33]. To explore if *CTNNB1* mutations occur in PNET, we enrolled 2 more cases of PNET that were diagnosed by surgery, but did not detect any mutations. Further analysis should be performed to determine if *CTNNB1* mutations occur in PNET.

One of the most important differential diagnoses of SPN is PNET[16,34]. Histologically, most SPNs show a solidmonomorphous growth in the peripheral parts of the lesion. In the center, tumor cells form pseudopapillary structures[35]. PNETs are morphologically very similar to SPNs. Immunostaining is useful to differentiate SPNs from PNETs. SPNs specifically express vimentin and CD10[8,36] and usually show focal immunoreactivity against synaptophysin but not for chromogranin A. On the other hand, PNETs usually show diffuse

staining for synaptophysin. Strong staining for chromogranin A is observed in differentiated neuroendocrine tumors, NETs but negative or very mild staining is found in poorly differentiated lesions[37,38]. ß-catenin localization is also quite different between these two tumor types. SPNs show cytoplasmic and nuclear staining[3,7], but PNETs show membranous staining. Accurate diagnosis of SPNs is sometimes difficult with EUS-FNA because of interpretative, sampling, and misclassification errors or insufficient material for immunostaining[19]. In the present study, 1 case of SPN could not be diagnosed pathologically on the basis of EUS-FNA samples. However, the *CTNNB1* mutation was detected by NGS, and the patient was diagnosed as having SPN and was scheduled for surgery at the time of reporting.

The current study was limited by two points. First, not all of the mutational analyses were performed prior to the final diagnosis by either EUS-FNA or surgery. Second, being a rare tumor, the sample size was rather small.

Conclusions

Analysis of exon 3 mutations in *CTNNB1* by NGS is feasible using EUS-FNA samples. All SPN cases showed *CTNNB1* mutations. Further exploration of mutational analyses including *CTNNB1* in neuroendocrine tumors is required to determine the genetic alterations of PNET.

Conflict of interest

The authors declare that they have no conflict of interest.

References

1. Papavramidis T, Papavramidis S. Solid pseudopapillary tumors of the pancreas: review of 718 patients reported in English literature. J Am Coll Surg 2005;200:965-72.
2. Frantz VK. Tumors of the pancreas. Atlas of tumor pathology, 1st series, Armed Forces Institute of Pathology: 1959: Washington DC.
3. Klimstra DS, Wenig BM, Heffess CS. Solid-pseudopapillary tumor of the pancreas: a typically cystic carcinoma of low malignant potential. Semin Diagn Pathol 2000;17: 66–80.
4. Yu PF, Hu ZH, Wang XB, et al. Solid pseudopapillary tumor of the pancreas : A review of 553 cases in Chinese literature. World J Gastroenterol 2010;16:1209-14.
5. Behrens J, Jerchow BA, Würtele M, et al. Functional interaction of an axin homolog, conductin, with beta-catenin, APC, and GSK3beta. Science 1998;280:596-9.
6. Aoki M, Hecht A, Kruse U, et al. Nuclear endpoint of Wnt signaling: neoplastic transformation induced by transactivating lymphoid-enhancing factor 1. Proc. Natl. Acad. Sci USA 1999;96:139-44.
7. Tanaka Y, Kato K, Notohara K, et al. Frequent ß-catenin Mutation and Cytoplasmic/Nuclear Accumulation in Pancreatic Solid-Pseudopapillary Neoplasm. Cancer Research 2001;61:8401-4.
8. Abraham SC, Klimstra DS, Wilentz RE, et al. Solid-pseudopapillary tumors of the pancreas are genetically distinct from pancreatic ductal adenocarcinomas and almost always harbor beta-catenin mutations. Am J Pathol 2002;160:1361-9.
9. Takahashi Y, Hiraoka N, Onozato K, et al. Solid-pseudopapillary neoplasms of the pancreas in men and women: do they differ? Virchows Arch 2006;448:561-9.
10. Liu BA, Li ZM, Su ZS, et al. Pathological differential diagnosis of solid-pseudopapillary neoplasm and endocrine tumors of the pancreas. World J Gastroenterol 2010;16:1025-30.

11. Wu J, Jiao Y, Dal Molin M, et al. Whole-exome sequencing of neoplastic cysts of the pancreas reveals recurrent mutations in components of ubiquitin-dependent pathways. Proc Natl Acad Sci USA 2011;108:21188–93.
12. Huang SC, Ng KF, Yeh TS, et al. Clinicopathological Analysis of beta-catenin and Axin-1 in Solid Pseudopapillary Neoplasms of the Pancreas. Ann Surg Oncol 2011;19(Suppl 3):S438–46.
13. Ross JS, Ali SM, Wang K, et al. Comprehensive genomic profiling of epithelial ovarian cancer by next generation sequencing-based diagnostic assay reveals new routes to targeted therapies. Gynecol Oncol 2013;130:554–9.
14. Nadler EP, Novikov A, Landzberg BR, et al. The use of endoscopic ultrasound in the diagnosis of solid pseudopapillary tumor of the pancreas in children. J Pediatr Surg 2002;37:1370-3.
15. Master SS, Savides T. Diagnosis of solid pseudopapillary neoplasm of the pancreas by EUS−guided FNA. Gastrointest Endosc 2003;57:965-9.
16. Bardales RH, Centeno B, Mallery JS, et al. Endoscopic ultrasound−guided fine−needle aspiration cytology diagnosis of solid pseudopapillary tumor of the pancreas: a rare neoplasm of elusive origin but characteristic cytomorphologic features. Am J Clin Path 2004;121:654-62.
17. Jani N, Dewitt J, Eloubeidi M, et al. Endoscopic ultrasound-guided fine-needle aspiration for diagnosis of solid pseudopapillary tumors of pancreas: a multicenter experience. Endoscopy 2008;40:200-3.
18. Maimone A, Luigiano C, Baccarini P, et al. Preoperative diagnosis of a solid pseudopapillary tumour of the pancreas by Endoscopic Ultrasound Fine Needle Biopsy: A retrospective case series. Dig Liver Dis 2013;45:957–60.
19. Hooper K, Mukhtar F, Li S, et al. Diagnostic error assessment and associated harm of

endoscopic ultrasound-guided fine-needle aspiration of neuroendocrine neoplasms of the pancreas. Cancer Cytopathol (e-pub ahead of print, 9 July 2013; doi:10.1002/cncy.21332)

20. Haba S, Yamao K, Bhatia V, et al. Diagnostic ability and factors affecting accuracy of endoscopic ultrasound-guided fine needle aspiration for pancreatic solid lesions: Japanese large single center experience. J Gastroenterol. 2013;48:973-81.
21. Eto K, Kawakami H, Kuwatani M, et al. Human equilibrative nucleoside transporter 1 and Notch3 can predict gemcitabine effects in patients with unresectable pancreatic cancer. Br J Cancer. 2013;108:1488-94.
22. Morin PJ, Sparks AB, Korinek V, et al. Activation of ß-catenin-Tcf signaling in colon cancer by mutations in ß-catenin or APC. Science 1997;275:1787-90.
23. Voeller HJ, Truica CI, Gelmann EP. ß-catenin mutations in human prostate cancer. Cancer Res 1998;58:2520-3.
24. Palacios J, Gamallo C. Mutations in the ß-catenin gene (CTNNB1) in endometrioid ovarian carcinomas. Cancer Res 1998;58:1344-7.
25. Miyoshi Y, Iwao K, Nagasawa Y, et al. Activation of the ß-catenin gene in primary hepatocellular carcinomas by somatic alterations involving exon 3. Cancer Res 1998;58:2524-7.
26. Liu C, Li Y, Semenov M, et al. Control of beta-catenin phosphorylation/degradation by a dual-kinase mechanism. Cell 2002;108:837-47.
27. Wu R, Zhai Y, Fearon ER, et al. Diverse mechanisms of beta-catenin deregulation in ovarian endometrioid adenocarcinomas. Cancer Res 2001;61:8247-55.
28. Wu G, Xu G, Schulman BA, et al. Structure of a beta-TrCP-1-Skp1-beta-catenin complex: destruction motif binding and lysine specificity of the SCF (beta-TrCP1) ubiquitin ligase. Mol Cell 2003;11:1445-56.
29. Angulo B, Conde E, Suárez-Gauthier A, et al. A Comparison of EGFR Mutation Testing

Methods in Lung Carcinoma: Direct Sequencing, Real-time PCR and Immunohistochemistry. PLoS One 2012;7:e43842.

30. Gerdes B, Ramaswamy A, Simon B, et al. Analysis of beta-catenin gene mutations in pancreatic tumors. Digestion 1999;60:544–8.
31. Jiao Y, Shi C, Edil BH, et al. DAXX/ATRX, MEN1, and mTOR pathway genes are frequently altered in pancreatic neuroendocrine tumors. Science 2011;331:1199–1203.
32. Kim JT, Li J, Jang ER, et al. Deregulation of Wnt/β-catenin signaling through genetic or epigenetic alterations in human neuroendocrine tumors. Carcinogenesis 2013;34:953–61.
33. Rinner B, Gallè B, Trajanoski S, et al. Molecular evidence for the bi-clonal origin of neuroendocrine tumor derived metastases. BMC Genomics 2012;13:594–602.
34. Vassos N, Agaimy A, Klein P, et al. Solid-pseudopapillary neoplasm (SPN) of the pancreas: case series and literature review on an enigmatic entity. Int J Clin Exp Pathol 2013;6:1051-9.
35. Adamthwaite JA, Verbeke CS, Stringer MD, et al. Solid pseudopapillary tumour of the pancreas: diverse presentation, outcome and histology. JOP 2006;7:635-42.
36. Notohara K, Hamazaki S, Tsukayama C, et al. Solid pseudopapillary tumor of the pancreas, immunohistochemical localization of neuroendocrine markers and CD10. Am J Surg Pathol 2000;24:1361-71.
37. Klöppel G, Rindi G, Anlauf M, et al. Site-specific biology and pathology of gastroenteropancreatic neuroendocrine tumors. Virchows Arch 2007;451:S9-27.
38. Klöppel G, Couvelard A, Perren A, et al. ENETS consensus guidelines for the standards of care in neuroendocrine tumors: towards a standardized approach to the diagnosis of gastroenteropancreatic neuroendocrine tumors and their prognostic stratification. Neuroendocrinology 2009;90:162–6.

Figure legends

Figure 1:

Histological features of solid-pseudopapillary neoplasm specimens obtained by endoscopic ultrasonography-guided fine-needle aspiration.

(a, b) Typical specimen (case 4). Small and uniform neoplastic cells have either eosinophilic or clear vacuolated cytoplasm. These loosely cohesive cells surround the delicate vessels and form pseudopapillae.

(c, d) Atypical specimen (case 7). The specimen contains a small number of neoplastic cells in the fibrous stroma that do not form apparent pseudopapillae. The small and uniform neoplastic cells have eosinophilic cytoplasm and show a plasmacytoid appearance. These clusters are difficult to distinguish from those of neuroendocrine tumors.

Fig. 1a

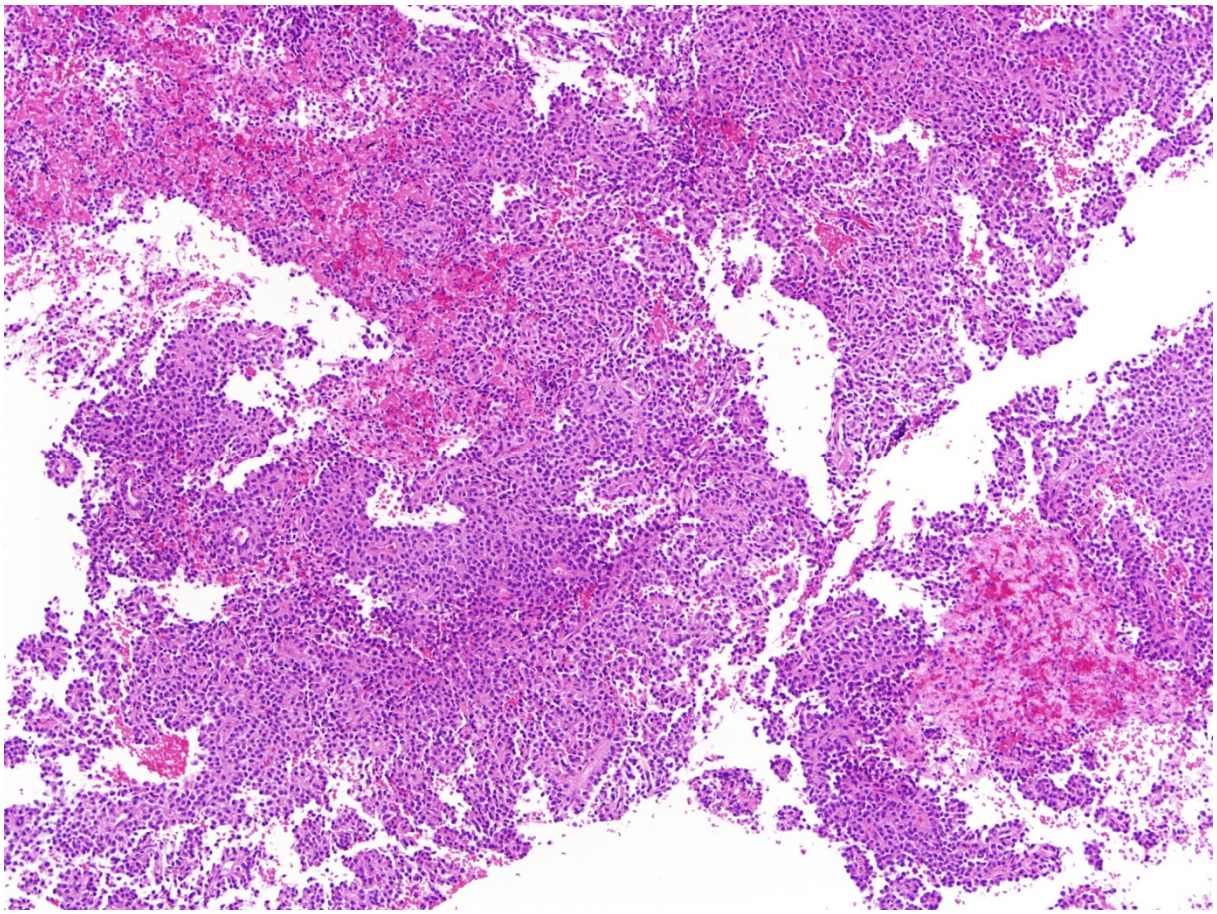

Fig. 1b

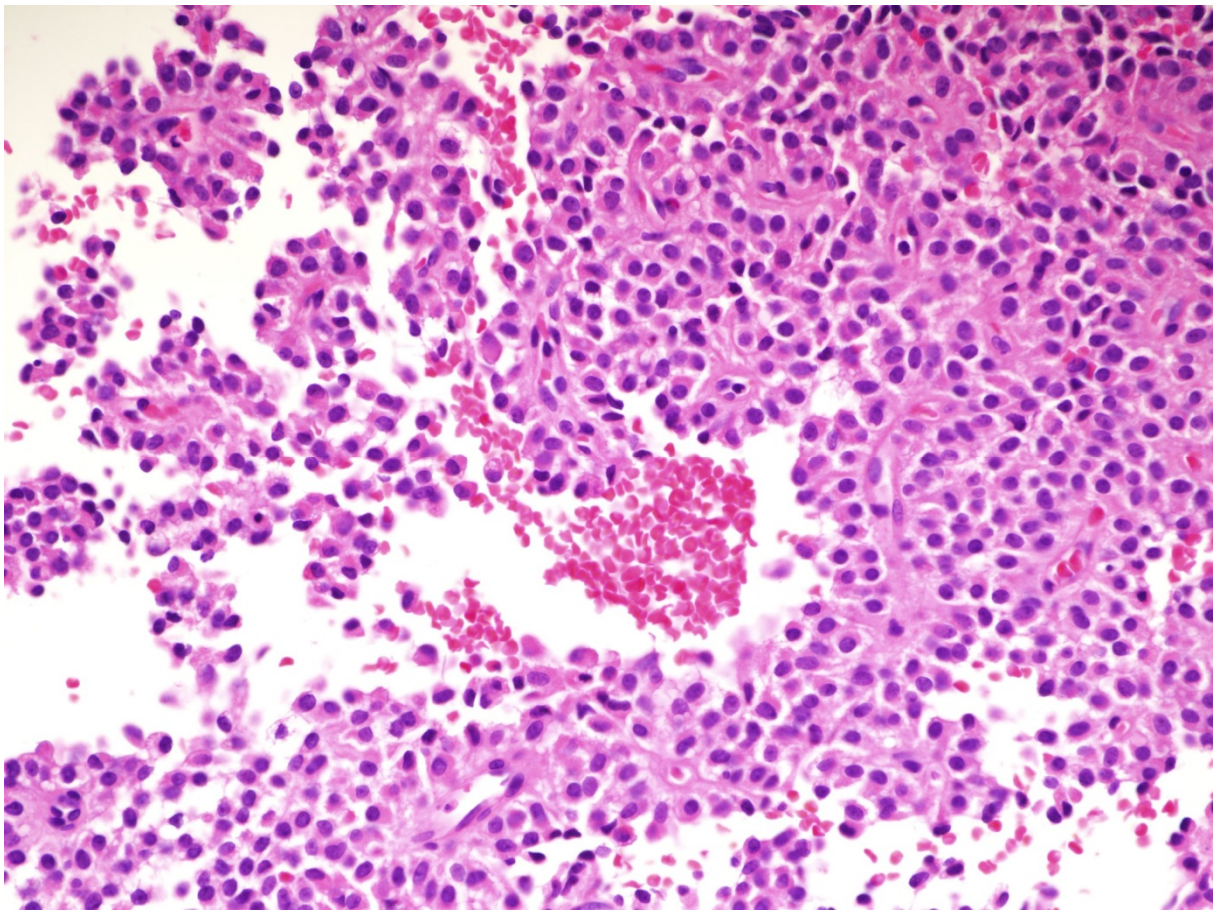

Fig. 1c

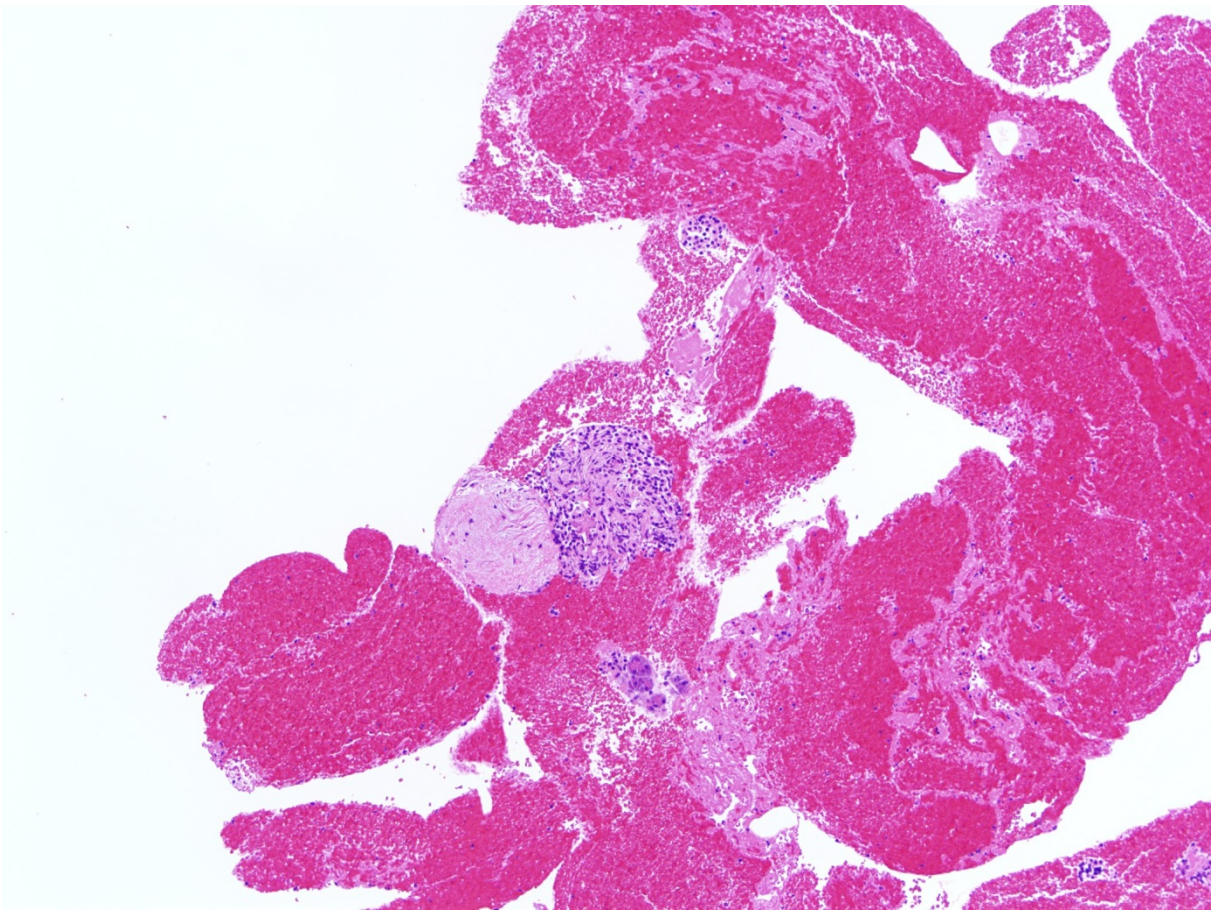

Fig. 1d

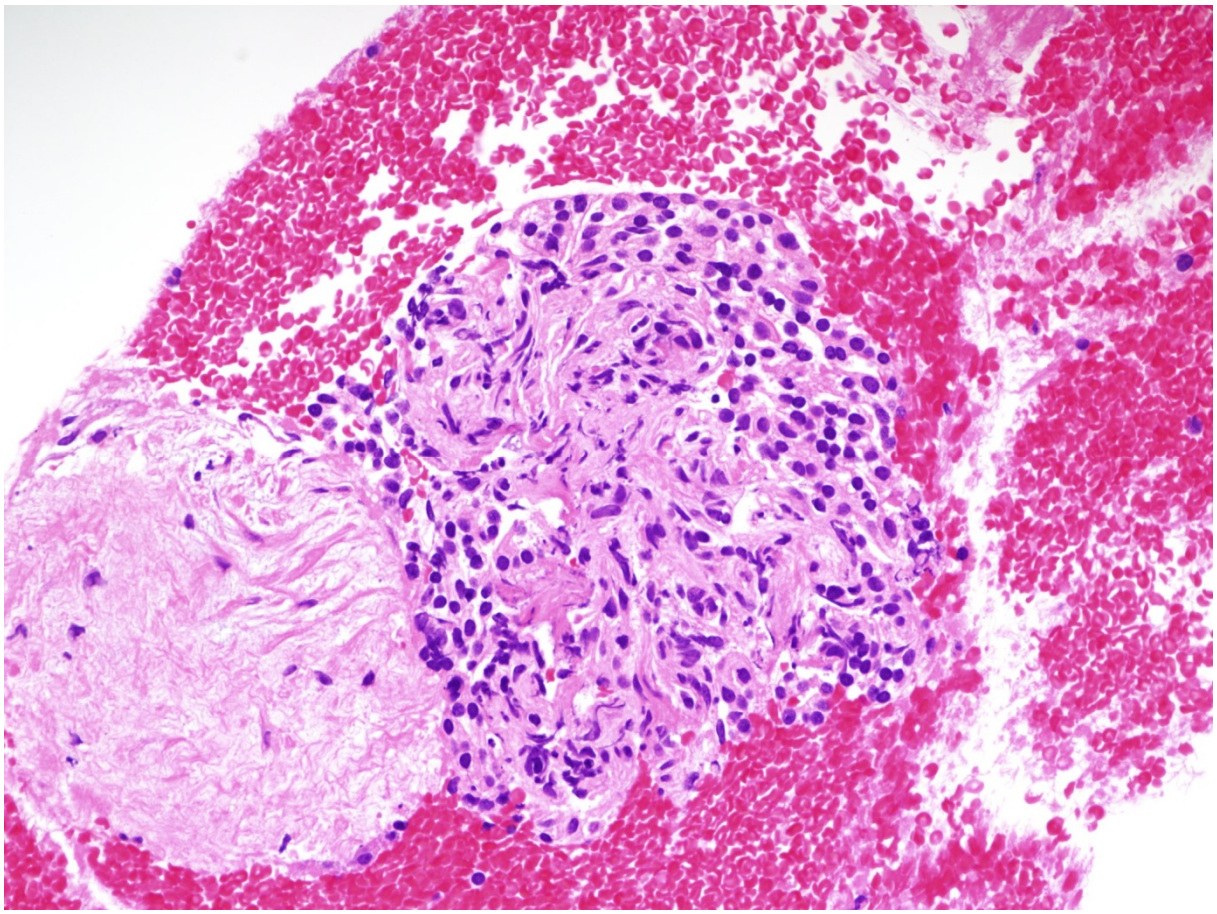

Table 1. Primers used in this study

Primers for the first PCR	
Forward	5′-CTGATTTGATGGAGTTGGACATGG-3′
Reverse	5′-CAGCTACTTGTTCTTGAGTGAAGG-3′
Primers for the second PCR (library preparation for next-geneartion sequencing)	
Primer pair for forward sequencing	
Forward	5′-CCATCTCATCCCTGCGTGTCTCCGACTCAG-barcode-CTGATTTGATGGAGTTGGACATGG-3′
Reverse	5′-CCTCTCTATGGGCAGTCGGTGATCAGCTACTTGTTCTTGAGTGAAGG-3′
Primer pair for reverse sequencing	
Forward	5′-CCATCTCATCCCTGCGTGTCTCCGACTCAG-barcode-CAGCTACTTGTTCTTGAGTGAAGG-3′
Reverse	5′-CCTCTCTATGGGCAGTCGGTGATCTGATTTGATGGAGTTGGACATGG-3′

Table 2. Clinicopathological Features

							Tumor markers				Results of immunohistochemical staining		
Case	Final diagnosis	Sex	Age	Location in pancreas	Tumor size (mm)	Radiological feature	CEA (ng/mL)	CA19-9 (IU/mL)	Procedure for the final diagnosis	Surgical procedure	CgA	Synaptophysin	ß-catenin
1	SPN	F	33	Pt	64	Solid/cystic	2	0	Surgery	DP	(-)	(+)	Nuclear
2	SPN	F	31	Pb	12	Solid/cystic	1	6	Surgery	Partial pancreatectomy	(-)	(-)	Nuclear
3	SPN	F	17	Ph	23	Solid/cystic	1	<1	Surgery	DpPHR	(-)	(+)	ND
4	SPN	F	36	Pbt	28	Solid/cystic	2	12	Surgery	DP	(-)	(+)	Nuclear
5	SPN	F	27	Pt	48	Solid/cystic	1	<1	Surgery	DP	(+)	(+)	Nuclear
6	SPN	F	13	Ph	63	Solid/cystic	1	9	Surgery	DpPHR	(+)	(+)	Nuclear
7	SPN	F	26	Pb	13	Solid	1	8	EUS-FNA	ND	(-)	(-)	ND
8	PDAC	F	64	Ph	33	Solid	10	3	Surgery	SSPPD	ND	ND	ND
9	PDAC	F	75	Pt	22	Solid	55	220	Surgery	DP	ND	ND	ND
10	PDAC	F	55	Ph	45	Solid	12	693	EUS-FNA	ND	ND	ND	ND
11	PDAC	M	62	Pt	70	Solid	79	>10,000	EUS-FNA	ND	ND	ND	ND
12	PDAC	F	76	Ph	70	Solid/cystic	4	>10,000	EUS-FNA	ND	ND	ND	ND
13	PDAC	M	64	Ph	17	Solid	22	53	EUS-FNA	ND	ND	ND	ND
14	PDAC	F	81	Ph	9	Solid	2	21	EUS-FNA	ND	ND	ND	ND
15	PDAC	F	78	Pt	66	Solid	12	361	EUS-FNA	ND	ND	ND	ND
16	PDAC	F	67	Ph	10	Solid	7	242	EUS-FNA	ND	ND	ND	ND
17	PDAC	M	63	Ph	27	Solid	7	2320	EUS-FNA	ND	ND	ND	ND
18	PDAC	M	57	Ph	17	Solid	6	30	EUS-FNA	ND	ND	ND	ND
19	PDAC	M	79	Ph	30	Solid	3	871	EUS-FNA	ND	ND	ND	ND
20	PDAC	M	44	Pbt	28	Solid	48	2880	EUS-FNA	ND	ND	ND	ND

Table 2. Continued

							Tumor markers				Results of immunohistochemical staining		
Case	Final diagnosis	Sex	Age	Location in pancreas	Tumor size (mm)	Radiological feature	CEA (ng/mL)	CA19-9 (IU/mL)	Procedure for the final diagnosis	Surgical procedure	CgA	Synaptophysin	ß-catenin
21	PDAC	M	78	Pt	27	Solid	3	229	EUS-FNA	ND	ND	ND	ND
22	PDAC	F	67	Ph	25	Solid	15	246	EUS-FNA	ND	ND	ND	ND
23	PDAC	M	80	Pt	47	Solid	440	>10,000	EUS-FNA	ND	ND	ND	ND
24	PNET	F	58	Pt	23	Solid	2	14	Surgery	DP	(+)	(+)	ND
25	PNET	M	51	Ph	52	Solid/cystic	2	31	Surgery	SSPPD	(+)	(+)	ND
26*	PNET	F	76	Lymph node	18	Solid	3	11	Surgery	Left nephrectomy	(+)	(+)	ND
27**	PNET	M	72	Pt	20	Solid	5	14	Surgery	DP	(+)	(+)	ND
28	PNET	F	58	Pb	18	Solid	2	14	Surgery	DP	(+)	(+)	ND
29	PNET	F	78	Ph	16	Solid	2	<1	Surgery	SSPPD	(+)	(+)	ND
30	PNET	M	79	Pb	9	Solid	3	8	EUS-FNA	ND	(+)	(+)	Membrane
31	PNET	F	69	Pt	8	Solid	3	5	EUS-FNA	ND	(+)	(+)	ND
32	PNET	F	77	Ph	17	Solid	2	47	EUS-FNA	ND	(+)	(+)	ND
33	PNET	F	45	Ph	17	Solid/cystic	3	26	EUS-FNA	ND	(+)	(+)	ND
34	PNET	F	62	Ph	10	Solid/cystic	6	40	EUS-FNA	ND	(+)	(+)	ND
35	Acinar cell carcinoma	M	46	Pbt	95	Solid/cystic	4	19	EUS-FNA	ND	(+)	(-)	ND
36	AIP	M	72	Pt	28	Solid	8	22	EUS-FNA	ND	ND	ND	ND
37	Focal pancreatitis	F	42	Pt	20	Solid/cystic	1	6	EUS-FNA	ND	ND	ND	ND
38	Focal pancreatitis	M	64	Ph	22	Solid	4	<1	EUS-FNA	ND	ND	ND	ND

SPN, Solid-pseudopapillary neoplasm; PDAC, pancreatic ductal adenocarcinoma; PNET, pancreatic neuroendocrine tumor; AIP, autoimmune pancreatitis; M, male; F, female; Ph, pancreatic head; Pb, pancreatic body; Pt, pancreatic tail; CEA, carcinoembryonic antigen; CA19-9, carbohydrate antigen 19-9; EUS-FNA, endoscopic ultrasound-guided fine-needle aspiration; DP, distal pancreatectomy; DpPHR, duodenum-preserving pancreas head resection; SSPPD, subtotal stomach-preserving pancreaticoduodenectomy; CgA, chromogranin A; ND, not done.

*The patient of case 26 developed a metastatic lymph node tumor 5 years after the initial surgery for PNET. Secondary surgery was left nephrectomy with metastatic lymph node tumor resection.
**The patient of case 27 had mixed ductal-neuroendocrine carcinoma and 2 synchronous PNETs.

Table 3. Mutations in *CTTNB1*

Case	Template	Mutated Codon	Nucleotide	AA substitution	Var Freq (%)	Coverage	Ref Cov	Var Cov	Direct seq
1	RNA	37	N378 C/A	Ser37Tyr	23.81	19047	14495	4535	Undetectable
2	RNA	32	N363 A/G	Asp32Gly	5.39	16072	15199	866	Undetectable
3	RNA	32	N362 G/C	Asp32His	48.77	25740	13161	12554	Undetectable
4	gDNA	41	N390 C/T	Thr41Tyr	31.07	4490	3093	1395	Undetectable
5	gDNA	37	N378 C/T	Ser37Phe	26.48	115799	84609	30665	Detectable
6	gDNA	41	N362 G/A	Asp32Asn	21.50	203919	43842	160077	Undetectable
7	RNA	41	N390 C/T	Thr41Tyr	29.68	35808	25167	10629	NA

AA, amino acid; Var Freq, variant frequency; Ref Cov, reference coverage; Var Cov, variant coverage; Direct seq, Direct sequencing; gDNA, genomic DNA; Ser, serine; Tyr, tyrosine; Asp, asparatic acid; Gly, glycine; His, histidine; Thr, threonine; Ile, isoleucine; Phe, phenylalanine; Asn, asparagine; NA, not available.